VARIABILITY OF MECHANICAL PROPERTIES OF CELLULAR LIGHTWEIGHT CONCRETE INFILL AND ITS EFFECT ON SEISMIC SAFETY

Nikhil P. Zade[1]; Avadhoot Bhosale[2], Prateek Kumar Dhir[3*]; Pradip Sarkar[4]; and Robin Davis[5]

[1]Ph. D Scholar, Department of Civil Engineering, National Institute of Technology Rourkela, Odisha 769008, India, Email: nikhilzade648@gmail.com.

[2]Department of Civil Engineering, Madanapalle Institute of Technology & Science, Madanapalle, Andhra Pradesh 517325, India, Email: avadhoot11@gmail.com.

[3*]Ph. D. Scholar at Department of Civil and Environmental Engineering, University of Strathclyde, Glasgow, UK, Email: prateek.dhir@strath.ac.uk (corresponding author)

[4]Professor, Department of Civil Engineering, National Institute of Technology Rourkela, Odisha 769008, India, Email: sarkarp@nitrkl.ac.in.

[5]Assistant Professor, Department of Civil Engineering, National Institute of Technology Calicut, NIT Campus P.O 673 601, Kozhikode, India, Email: robin@nitc.ac.in.

This is a peer-reviewed, accepted author manuscript of the following article: Zade, N. P., Bhosale, A., Dhir, P., Sarkar, P., & Davis, R. (2021). Variability of mechanical properties of cellular lightweight concrete infill and its effect on seismic safety. Natural Hazards Review. https://doi.org/10.1061/(ASCE)NH.1527-6996.0000501

Abstract

Cellular lightweight concrete (CLC) block masonry has gained popularity in the masonry market with the growing demand in the modern construction industry due to its various advantages, including a positive impact on the environment. Subsequently, the detailed characterization of its vital engineering properties should be studied for the development of the mathematical model, analysis, evaluation, and design of structures made of CLC block masonry. The present study investigates the variability in two important strength properties of CLC block masonry and proposes the most appropriate models for their statistical distribution to support probability-based structural analysis and design. This study shows that the assumption of a normal distribution in the absence of an appropriate uncertainty model can result in an inaccurate estimate of the seismic risk of an RC frame building infilled with CLC block masonry. The paper further assesses the seismic safety of a typical RC framed building infilled with CLC block masonry in relation to traditional brick masonry, considering the proposed uncertainty model. It is observed that although CLC block masonry results in a higher seismic risk compared to traditional brick masonry, it can be used as an infill material in high seismic areas, as it results in a probability of failure within the acceptable limit.

Keywords: CLC, compressive strength, shear-bond strength, uncertainty; goodness-of-fit test, seismic risk.

INTRODUCTION

Rapid economic growth in the construction industry can be seen in almost all developing countries, where brick remains as one of the essential building materials. About 340 billion tons of clay was consumed by the Indian brick industry in 2006 for producing 180 billion tons of clay bricks (Rasheed, 2018). The development of environmental-friendly materials to replace natural resources in the construction industry has received significant attention in recent years. In that line, the cellular lightweight concrete (CLC) block is gaining popularity in the construction industry as an infill masonry material due to its wide range of advantages over clay brick with eco-friendly nature. Low density, smooth surfaces, fire resistance, better

workability, and better thermal-insulation capabilities are some of the vital benefits of CLC block masonry. Lower values of mass density and elastic modulus of CLC block tend to reduce the inertia forces on the building induced by the seismic motion (Bhosale *et al.,* 2020). Detailed information on the composition and manufacturing process of CLC blocks is available in RILEM (1993).

Strong research output on the performance of structures made of CLC block masonry will increase the confidence of stakeholders to increase the use of CLC blocks in the masonry construction industry and thus increase the conservation of natural resources. However, a detailed literature review did not reveal any studies on performances of structures made from CLC blocks. The performance and safety of a structure are directly dependent on the uncertainty associated with the material properties. Ignoring such uncertainties despite the advancement of available computer technology will make structural analysis less satisfactory and less realistic. Descriptions of uncertainties for traditional building materials such as structural concrete, steel rebar, clay, and fly-ash brick masonry are available in an ample amount (Sahu *et al.,* 2019, 2020; Sahoo *et al.,* 2020; Kilinc *et al.,* 2012; Stewart and Lawrence 2007; Aryana 2006; Schueremans, 2001). However, similar studies on the uncertainty modelling of CLC block masonry did not receive any research attention. Most of the studies (Bhosale *et al.,* 2020; Rasheed, 2018; Aliabdo *et al.,* 2014; Yue and Bing, 2014; Chen *et al*., 2014; Jos and Lukito, 2011; Jones and McCarthy, 2005; Kearsley and Wainwright, 2002) on the CLC block masonry are limited only to the characterisation of its physical and mechanical properties.

The present study aims to evaluate the seismic performance of CLC block infilled RC framed buildings considering the uncertainties inherent in structural capacities and loading. To accomplish this objective, a series of laboratory experiments are conducted to develop the uncertainty and nonlinearity models of CLC block masonry assemblages. Most suitable probability distribution functions to describe the uncertainties in the compressive and shear-bond strength of CLC block masonry are obtained from the statistical analyses of experimental results. The nonlinear model of CLC block masonry required for the structural analyses is obtained by combining the experimentally obtained strength parameters and a widely used backbone curve for masonry infill (Fardis, 1996).

RESEARCH SIGNIFICANCE

The use of CLC block masonry as infill material in RC framed buildings has gained attention these days due to its several advantages over traditional brick masonry. Consequently, many studies have been conducted in the past on the physical and mechanical properties of CLC block masonry. However, the performance of structures made of CLC block masonry has not been reported in the published literature. Comprehensive research output in this facet will increase the stakeholder confidence and enhance the practical usage of this masonry material. This paper reports two very important aspects of CLC block masonry: (a) quantifying the variability associated with compressive and shear-bond strength of CLC block masonry to support probability-based structural analysis and (b) the seismic safety of RC framed building infilled with CLC block masonry relative to traditional brick masonry which can form a basis for choosing the infill material in terms of its seismic resistance.

EXPERIMENTAL PROGRAM AND TEST RESULTS

Past studies (Bhosale *et al.,* 2018 and Sahu *et al.,* 2020) have reported that the compressive and shear-bond strength of infill masonry plays an essential role in seismic performance. Accordingly, an experimental program is carried out to evaluate the compressive and shear-bond strength of CLC block masonry and the associated uncertainty. Published literature and standards have not recommended specific guidelines for the experimental assessment for strength properties of CLC block masonry. Therefore, the endorsement of ASTM C1314 (2018) and BS EN 1052-3 (2002) are considered in the present study for compressive and shear-bond strength tests, respectively. Consequently, a three-course stack bonded triplet specimen with a height-to-thickness ratio of 3.4 that satisfies the requirements of these two standards is considered for the evaluation of two selected strength properties. Commercially procured CLC blocks (Fig. 1) of size 600 × 200 × 100 (± 5 mm) are cut using a diamond blade cutter into brick sizes of 200 mm × 100 mm × 100 mm to prepare the CLC block masonry specimens. Commercially available block adhesive confirming to ANSI A118.4 (2019) is used as a binder.

Twenty triplet specimens are prepared for each of the two strength tests. Photographs of typical CLC block masonry triplets are presented in Fig. 2. CLC block masonry triplets are tested under uniaxial compression in a load-controlled compression testing frame, as shown in Fig. 3(a). The maximum load before failure divided by the cross-sectional area gives the compressive strength of masonry (f_m) triplet.

The shear-bond strength of the masonry specimen is evaluated as per BS EN 1052-3 (2002) without any pre-compression using a load-controlled compression testing frame. The triplet specimen is supported on two outer blocks, and the compression load is applied gradually on an unsupported central block (Fig. 3b). The load is applied until the bond between the blocks is failed. Total load before failure divided by two times the cross-sectional area of joint gives the shear-bond strength (τ_{cr}) of masonry triplets.

Statistics and percentile values of the strength data obtained experimentally are presented in Table 1. Figs. 4-5 presents the histogram of compressive and shear-bond strength data for all the specimens tested. Two modes of failure, namely face shell separation and shear break, can roughly describe the failure of masonry assemblages detected during the compression test. During the experimental evaluation of shear-bond strength, failure depends on the relative strength of the CLC block unit and the bonding adhesive. Accordingly, two types of failure patterns are detected in the masonry specimens during the shear-bond test: (a) failure through the CLC units when the CLC block is weaker and (b) failure through the block adhesive bond when the bond is weaker than the CLC block.

DEVELOPMENT OF VARIABILITY MODELS

Design and safety assessment of structures made of CLC block masonry requires probabilistic models that describe the variability of its mechanical properties. This section focuses on the representation of the variability of compressive and shear-bond strength using different probability distribution models. Experimentally obtained compressive and shear-bond strength data are used to develop the probability distribution models utilizing the statistical goodness-of-fit (GOF) tests.

Normal, Lognormal, Gamma, Weibull, Gumbel max and Gumbel min are the pre-decided two-point standard probability distribution models which are selected in this study as these distributions are reported

(Sorrentino *et al.,* 2016; Montazerolghaem, 2015; Lawrence, 1985) to be describing the strength properties of brittle materials better. Specific GOF tests such as Kolmogorov-Smirnov (KS), Anderson Darling (AD), and Chi-Square (CS) are used in the present study. The KS test is widely used for the analysis of continuous distributions and is reported to be independent of sample size. However, KS tends to be more sensitive near the middle of the distribution than at the tails (Sahu *et al.,* 2020). AD is a modification of the KS test and is more sensitive to the tail region (Stephens, 1974). Similarly, when a large number of random variables are used, the CS test is found to be more efficient.

The selection criterion for the best-fit distribution is based upon the total statistics, which is defined as the square root of the sum of the squares of individual test statistics obtained from three GOF tests. The lowest value of the total statistics corresponds to the lowest rank and presents the best-fitted distribution model. For each probability distribution function, the test statistic is determined and ranked based on the statistic value in line with the methodology followed by previous studies (Chandrappa and Biligiri, 2017; Chen *et al.,* 2014; Kilinc *et al.,* 2012). Commercial software EasyFit Professional (version 5.6) is used for all the statistical analyses. Table 2 presents the appropriate statistical distribution functions generated for the compressive and shear-bond strength properties of the CLC block masonry.

The results of the GOF tests for compressive and shear-bond strength of CLC block masonry assemblages are reported in Tables 3-4. The cumulative distribution functions for the test data for each of the selected distribution models are presented in Fig. 6. It can be observed from Table 3 that for compressive strength of CLC block masonry, KS has minimum statistics for Gamma distribution, AD has minimum statistics for normal distribution, and CS has minimum statistics for the Gumbel max distribution. All three selected GOF tests are not in agreement with one single distribution model for the variability description of the compressive strength of CLC block masonry. Hence, the selection of the best-fitted distribution is carried out based on minimum total statistics value. Similar observations can be made from Table 4 for the variability of shear-bond strength. Based on minimum total statistics value, Gamma and Gumbel max are found to be the best-fitted distribution for compressive and shear-bond strength of CLC block masonry, respectively. As observed, there is a small difference in the total statistic values of first ranked and some

other higher ranked distributions. Also, the relative statistic values presented in this study may alter if the data pool is changed. Therefore, any of the higher-ranked distributions with low total statistics values may be considered to describe the variability in the strength properties of CLC block masonry.

SEISMIC PERFORMANCE EVALUATION

The effect of the variability in masonry strength on the seismic performance of infilled RC framed buildings is identified as one of the primary objectives of this study. A probability-based seismic evaluation method (Vamvatsikos and Cornell, 2002) using incremental dynamic analysis (IDA) is employed for this purpose. The seismic performance is evaluated through probabilistic seismic demand models (PSDM), fragility curves, drift hazard curves, and the probability of unacceptable behaviour (P_{PL}). The fragility function represents the probability of demand parameter (D) exceeding the selected limit state capacity of the structure (C) at a chosen intensity measure (IM). It can be expressed in the closed-form (Celik and Ellingwood, 2010) as follows:

$$P(C \le D|IM) = \Phi\left(\frac{\ln(\hat{D}) - \ln(\hat{C})}{\sqrt{\beta_{D|IM}^2 + \beta_c^2 + \beta_m^2}}\right) \quad (1)$$

Where Φ is the standardized Gaussian cumulative distribution function, $\hat{D}$ and $\hat{C}$ are the median values of D and C respectively; $\beta_{D|IM}$, β_c, and β_m are the dispersions in D (at a given IM), C, and structural model, respectively. The $\hat{D}$ is considered as per Cornell *et al.* (2002), where a power-law relationship is assumed to exist between demand parameter and seismic intensity measure as follows.

$$\hat{D} = a\,(IM)^b \quad (2)$$

Where a and b are the constant coefficients. This power-law describes the PSDM of the building under consideration. The median values of limit state capacities ($\hat{C}$) are considered from the published literature. The value of β_c is assumed to be 0.25 as per ATC 58 (2012), considering the fair quality of construction, and β_m is assumed to be $0.25\sqrt{2}$ as per Mistri *et al*. (2019).

The seismic evaluation is further extended by incorporating the site hazard. Seismic hazard is an important parameter to predict the likelihood of the unacceptable behavior of a selected RC frame at a given site. In the present work, a second-order approximation (Vamvatsikos, 2013) of the hazard curve, $H(IM)$ around the region of interest is chosen as follows:

$$H(IM) = k_0 \exp\left[-k_2 \ln^2(IM) - k_1 \ln(IM)\right] \quad (3)$$

Where k_0, k_1 and k_2 are the constant coefficients. The drift hazard function, $H_D(d)$, measures the annual probability that D exceeds any specified value (d), which can be obtained by combining the hazard curve and the PSDM. If the cumulative annual probability of occurrence of an earthquake of given intensity ($IM = x$) is defined by hazard function, $H(IM)$, then the probability of exceedance of demand can be obtained by conditioning on all possible levels of the ground motion using the theorem of total probability (Benjamin and Cornell, 2014) as follows:

$$H_D(d) = \int P[D \geq d | IM = x] \left| dH(x) \right| \quad (4)$$

Where $dH(x)$ can be obtained from the hazard curve, $H(IM)$. Incorporating PSDM (Eq. 2) and the second-order power-law approximation of hazard curve (Eq. 3), the simplified form of the drift hazard function can be expressed as follows:

$$H_D(d) = P[D \geq d] = \sqrt{q}\, k_0^{1-q} H(IM^d) \exp\left[\frac{k_1^2}{4k_2}(1-q)\right] \quad (5)$$

Where IM^d is the intensity measure consistent with the drift level, $\hat{D} = d$ and can be calculated as per Eq. (6). The constant q can be calculated as per Eq. (7).

$$IM^d = \left(\frac{d}{a}\right)^{1/b} \quad (6)$$

$$q = \left(\frac{b^2}{b^2 + 2k_2 \beta_{D|IM}^2}\right) \quad (7)$$

189 The probability of unacceptable behaviour (P_{PL}) gives the seismic risk of buildings at a given limit state in
190 a quantitative manner. The P_{PL} can be calculated by relating the $H_D(d)$ and chosen limit state capacity.
191 Using the total probability theorem, P_{PL} can be defined as:

192 $$P_{PL} = P[C \le D] = \sum_{all\, d_i} P[C \le D \mid D = d_i]\, P[D = d_i] \tag{8}$$

193 Considering the second-order power-law approximation of hazard curve, Vamvatsikos (2013) has given a
194 simplified equation to calculate P_{PL} as follows:

195 $$P_{PL} = \sqrt{\phi}\; k_0^{1-\phi} [H(IM^{\hat{C}})]^{\phi} \exp\left[\frac{k_1^2}{4k_2}(1-\phi)\right] \tag{9}$$

196 where, the constant ϕ and the intensity measure corresponding to $\hat{C}$, $IM^{\hat{C}}$ can be obtained from Eq. (10)
197 and Eq. (11) respectively:

198 $$\phi = \frac{b^2}{b^2 + 2k_2(\beta_{D|IM}^2 + \beta_c^2)} \tag{10}$$

199 $$IM^{\hat{C}} = \left(\frac{\hat{C}}{a}\right)^{1/b} \tag{11}$$

200 **STRUCTURAL MODELLING**

201 A typical RC infilled framed building (Fig. 7a) with eight storeys of 3.2 m of uniform height and four bays
202 of 5 m of uniform width (8S4B) is selected for the present study. This building configuration is used as a
203 benchmark building in many previous studies (Dhir *et al.,* 2020; Bhosale *et al.,* 2018). The building is
204 assumed to be infilled with 230 mm thick masonry. Two traditional infill masonry materials (fired clay and
205 fly-ash brick) are considered for the present study in addition to CLC block masonry. The buildings are
206 designed as per relevant Indian standards (IS 1893: 2016; IS 456: 2000) for seismic force corresponding to
207 a peak ground acceleration (PGA) of 0.36g. The infill masonry material alters the mass and stiffness
208 properties of the structure and hence influences the design base shear. The maximum design base shear
209 obtained out of the three considered infill masonry is used for the design of RC members, and the design
210 details remain uniform for all frames considered in this study. Characteristic compressive strength of

concrete (f_{ck}) and yield strength of reinforcement steel (f_y) are considered as 25 MPa and 415 MPa, respectively. Table 5 provides the cross-section and reinforcement details of RC elements of the buildings. The buildings are modelled and analysed using Open System for Earthquake Engineering Simulation (OpenSEES) laboratory tool developed by McKenna *et al.* (2016) for the nonlinear time history analysis. The spread plasticity model is considered for the force-based nonlinear beam-column fiber elements. The infill wall is modelled as a double bracing compression-only diagonal strut element which uses backbone purely in compression as per Celarec *et al.* (2012). The equivalent width of a diagonal strut is calculated as per the recommendation of IS 1893 (2016). It can be seen from Fig. 7(b) that the following six parameters are necessary for completely defining the backbone curve of the diagonal strut: F_{max}, F_{cr}, F_{res}, K_{sec}, K_{el}, and K_{deg}. All of these parameters are evaluated using the compressive and shear-bond strength of infill masonry given in Table 6, the elastic modulus values are given in Table 7, and the geometric dimensions of the infill panel. The relationship given by Basha and Kaushik (2015) is used to obtain the shear modulus of masonry infill from the experimentally evaluated shear-bond strength. Further details about the approach of modelling the infill masonry used in the present study can be available elsewhere (Celarec *et al.,* 2012; Fardis, 1996).

The modelling approach considered in this study is validated with the experimental results of an infilled frame subjected to a pseudo-static cyclic load available in published literature (Crisafulli, 1997). Details of the frame dimensions, material properties, and loading sequence are available in Crisafulli (1997). Fig.8 shows the comparative plot of the base shear force versus the lateral roof displacement obtained from the experiment and the analysis considering the adopted modelling approach. This figure shows that the results of the analysis are quite consistent with the experimental results that confirm the validity of the modelling approach used in the present study.

It is to be noted that, as 2D building models are considered, the torsional effects and out-of-plane response of the masonry infill are ruled out in the present study. As the ground motion records for the Indian regions are limited, the accelerograms recorded in the California region (FEMA P695: 2009) are adopted in the present study to have a statistically sufficient number of ground motions. Accordingly, 22 pairs (44 ground

motions) of far-field ground motions of the California region are selected for modelling the uncertainty in seismic loading. Fig. 9 presents the response spectra of the selected ground motions at 5% damping. General characteristics of selected ground motions are as follows: magnitude > 6.5 in Richter scale, distance from source to site > 10 km, PGA > 0.2g, and peak ground velocity > 15 cm/s.

The uncertainty in the strength properties of the building is modelled using the variability of selected masonry materials as described in Table 6. The properties of the clay and fly-ash brick masonry are taken from the published literature, whereas the same for CLC block masonry are experimentally evaluated. It can be noted that in the absence of an appropriate variability model for any material, a normal distribution is often assumed in probability-based seismic analysis. Therefore, an assumed normal distribution for the strength parameters of CLC block masonry is additionally considered as a reference. The material properties of RC frames are kept at their characteristic values. The mass density, the elastic modulus of all the materials considered in this study are presented in Table 7. The seismic weight (W), the elastic period of the first mode of vibration (T_1) from OpenSEES analysis, and design base shear (V_b) by the equivalent static method as per IS 1893 (2016) for the infilled RC frame modelled with the mean values of selected infill masonry (Table 7) are shown in Table 8. CLC infill masonry has lower compressive strength, shear-bond strength, mass density, and elastic modulus in comparison with traditional infills (clay, fly-ash), as indicated in Tables 6-7. Low seismic weight and low base shear of the building frame are observed for the case of CLC block masonry due to its low density and elastic modulus. However, it is found that the selected infill masonry materials do not affect the fundamental period of the building structure significantly, as the combined effect of mass and stiffness of the three infill masonry materials are approximately equal. Lower compressive and shear-bond strength negatively affects the seismic performance of CLC block infilled RC framed building, while lower mass density and elastic modulus attract lesser seismic force on it. The above mechanical properties will collectively affect the seismic performance of CLC block infilled building. Pushover analyses are carried out for the selected building frames considering fundamental mode shape vector and the mean values of relevant material properties to have an in-depth quantitative comparison of

its seismic behavior. Pushover curves presented in Fig. 10 show that the CLC block infilled frame has considerably lower strength and stiffness when compared with traditional infill materials.

ASSESSMENT OF THE SEISMIC PERFORMANCE

The selected infilled RC building frames are analysed using the probability-based methodology described in the earlier section. In the present study, the spectral acceleration at the first mode of vibration ($S_{a,T1}$) is considered as the seismic intensity measure, and maximum interstorey drift observed among all the storeys of the building during the earthquake (ISD) is considered as the demand parameter. Three performance limit states for RC moment-resisting infilled frame are considered from published literature (Bhosale et al., 2018; Mamun and Saatcioglu, 2017; Haran et al., 2015; ASCE/SEI 41: 2013, ACI 374.2R: 2013 FEMA 356: 2000) as follows: immediate occupancy (IO) at ISD = 1%, life safety (LS) at ISD = 2%, and collapse prevention (CP) at ISD = 4%. A total of 44 computational models of the building frame are generated for each of the three infill masonry material categories through the sampling of selected input variables (Table 6). Selected 44 ground motions are linearly scaled from a PGA of 0.1g to 1.0 g, and nonlinear time history analyses (NLTHA) are conducted for each of the 44 building models considering a randomly selected earthquake to obtain maximum ISD. As discussed earlier, the building performance is assessed in terms of PSDM, fragility curve, drift hazard curve, and P_{PL}. The analytical outcomes of the present study are discussed below.

PSDMs

The maximum ISD obtained from NLTHA and the $S_{a,T1}$ of the corresponding ground motion is plotted, and the power-law relationship between these two parameters, which represents the PSDM of the selected building, is developed through regression analysis. Fig. 11 presents the PSDMs of the CLC block masonry infilled building frame considering two variability models: (a) proposed best-fitted distribution (BF) and (b) assumed normal distribution (ND). Fig. 11 shows that ND results in higher values of ISD of the building frame when compared with BF distribution. A higher value of ISD corresponds to the higher vulnerability of the buildings. Fig. 12 presents the PSDMs of the building models infilled with three selected masonry

materials, showing that CLC block masonry results in the highest drift demand among others. The regression coefficients *a* and *b* (Eq. 2) and $\beta_{D|IM}$ for all the PSDMs are presented in Table 9.

Fragility Curves

The seismic performance of selected building frames is further analyzed through fragility curves at different performance limit states and presented in Fig. 13. This figure shows that the ND results in the higher vulnerability of CLC infilled frame compared to that of BF distribution, which indicates that the assumption of ND can be conservative in the seismic risk analysis of CLC infilled RC framed building. Fig. 13 further shows that the CLC block masonry results in the most vulnerable seismic performance of the infilled frame when compared with other traditional brick masonry. This may be attributed to the low compressive and low shear-bond strength of CLC block masonry among the selected infill materials, which ultimately reduces the lateral strength of the CLC infilled frame during seismic excitation.

It should be noted here that the $S_{a,T1}$ used in the PSDMs and the fragility curves (Figs. 11-13) corresponds to the structure-specific first mode period of vibration. In such a situation, it may not be appropriate to directly compare the seismic responses of the different frames on the same plot, as each $S_{a,T1}$ represents a different *IM*. However, the purpose of these figures is to have a visual comparison in line with some of the published literature (Wijaya *et al.,* 2020; Bhosale *et al.,* 2018). It can also be seen that the first mode periods of the three selected building frames are not very different. For a legitimate comparison, the fragility percentiles for selected RC frames infilled with different masonry materials are presented in Table 10. It can be seen that this table supports all the conclusions drawn from Figs. 11-13.

Drift Hazard Curves

The true evaluation of the building's seismic performance must consider the seismic hazard of the selected site. Accordingly, the drift hazard curves of the selected building models are developed considering the seismic hazard of the Guwahati region (India) with similar conditions (magnitude, distance from the source, rupture process, travel path from source to site, and local site conditions) that of California region. The

PGA seismic hazard curve of the Guwahati region developed (Nath and Thingbaijam, 2012) based on probabilistic seismic hazard analysis (PSHA) is first converted into a pseudo-acceleration hazard curve using a uniform hazard response spectrum and then fitted to the second-order form of the Eq. (3). The hazard curves are developed in the present study for each of the selected infilled frames corresponding to their first mode periods. Fig. 14 presents a typical $S_{a,T1}$ hazard curve at Guwahati, India, for CLC block masonry infilled frame (T_1 = 0.67 s). The drift hazard curves developed for different cases of the building are shown in Fig. 15.

It is found that Fig. 15 endorses the conclusions of PSDM and fragility analyses. The order of building frame infilled with various masonry materials in terms of increasing drift hazard is found to be CLC_ND > CLC_BF > Fly-ash > Clay.

Mean Annual Probability of Exceedance

The annual probability of collapse or the annual exceedance probability of the selected frame infilled with different masonry materials at various performance limit states is calculated and presented in Table 11. The P_{PL} of the building infilled with different masonry materials relative to that of CLC block masonry with BF distribution is computed and presented in the parentheses to assess the relative vulnerability. This table concludes that CLC block masonry results in a higher probability of collapse in infilled RC framed buildings in comparison with traditional brick masonry. The difference in the probability of collapse is in the range of 10-20% for clay and fly-ash brick masonry with respect to CLC block masonry. However, the probability of collapse of the RC frame building infilled with CLC block masonry estimated considering a hazard curve representative of the highly active seismic zone of India is found to be within the acceptable limits of the design code. Therefore, CLC block masonry can be safely used as infill material in high seismic areas. It also concludes that the normality assumption of the strength properties of CLC block masonry can lead to an error of about 5-10% in the probability of collapse.

SUMMARY AND CONCLUSIONS

The present study assesses the variability in two important strength properties of CLC block masonry by performing goodness-of-fit tests using limited sets of experimental data and considering the two-parameters probability distribution functions. The most appropriate statistical distribution that closely fits the observed data set is suggested for the compressive and shear-bond strength of CLC block masonry. This result can be used as an essential input for the reliability-based analysis and design of CLC block masonry structures. This study compares the seismic response of a typical CLC block masonry infilled RC frame obtained considering the assumed normal distribution and proposed best-fitted distribution of input strength properties of CLC block masonry and concludes that the consideration of the appropriate distribution function is vital for the precise estimation of seismic risk.

Further, the seismic risk of a benchmark infilled RC frame is evaluated in terms of PSDM, fragility curve, drift hazard, and $P_{PL,}$ incorporating the proposed distributions of masonry strength properties. The results of CLC block masonry relative to two traditionally used masonry materials (clay and fly-ash brick) are presented, which concludes that CLC block masonry results in the most vulnerable seismic performance of the infilled frame when compared with other traditional brick masonry. This may be attributed to the lowest shear-bond strength of CLC block masonry among the selected infill materials. However, the probability of collapse of the RC frame building infilled with CLC block masonry estimated considering a hazard curve representative of the highly active seismic zone of India is found to be within the acceptable limits of the design code. Also, the use of CLC block over traditional brick masonry has certain economic and environmental benefits. The large size and smooth surface of CLC blocks reduce material requirements for plastering and packing while improving the speed of construction and workability. Better fire resistance and thermal insulation are predefined advantages of CLC masonry in building construction. The use of CLC block masonry in the construction industry reduces the impact on the environment by conserving natural resources. The results presented in this paper will help to choose the appropriate masonry materials for the construction of infilled frames. Nevertheless, a cost-benefit analysis including environmental impact may be required to suggest the suitability of CLC block masonry in the infilled framed building precisely.

366 It should be noted here that the conclusions presented in this paper are based on the results of a typical
367 infilled frame with far-field seismic ground motion records from one region under certain modeling
368 assumptions. Further experimental and analytical studies with a robust modeling approach on a statistically
369 significant number of building models may be required to endorse this finding.
370

371 **DATA AVAILABILITY STATEMENT**

372 Some data, models, or codes generated or used during the study are available from the corresponding
373 author by request (OpenSEES modeling files and generated outputs).
374

375 **REFERENCES**

376 ACI 374.2R (2013). "Guide for testing reinforced concretestructural elements under slowly applied
377 simulated seismic loads". American Concrete Institute, ACI committee 374. Michigan, United States.
378 Aliabdo, A. A., Abd-Elmoaty, A. E. M., and Hassan, H. H. (2014). "Utilization of crushed clay brick in
379 cellular concrete production." *Alexandria Engineering Journal*, 53(1), 119-130.
380 ANSI A118.4 (2019). "American national standard specifications for modified dry-set cement mortar".
381 American National Standard Institute, The Council of America.
382 Aryana S. A. (2006). "Statistical analysis of compressive strength of clay brick masonry prisms." M.S.
383 Thesis, Dept. of Civil Engineering, Univ. of Texas.
384 ASCE/SEI 41 (2013). "Seismic evaluation and retrofitof existing buildings". American Society of Civil
385 Engineers, Varginia, United States.
386 ASTM C1314 (2018). "Standard test method for compressive strength of masonry prism." American
387 Society for Testing and Materials, West Conshohocken, PA.
388 ATC-58 (2012). "Guidelines for seismic performance assessment of buildings." Applied Technology
389 Council. Redwood City, CA.
390 Basha, S. H., and Kaushik, H. B. (2015). "Evaluation of nonlinear material properties of fly ash brick
391 masonry under compression and shear." *Journal of Materials in Civil Engineering*, 27(8), 04014227.
392 Basha, S. H., and Kaushik, H. B. (2016). "Suitability of fly ash brick masonry as infill in reinforced concrete
393 frames." *Materials and Structures*, 49(9), 3831-3845.
394 Benjamin, J. R., and Cornell, C. A. (2014). "Probability, statistics, and decision for civil engineers."
395 McGraw-Hill, New York.

Bhosale, A. S., Davis, R., and Sarkar, P. (2018). "Seismic safety of vertically irregular buildings: Performance of existing indicators." *Journal of Architectural Engineering*, 24(3), 04018013.

Bhosale, A., Zade, N. P., Sarkar, P., and Davis, R. (2020). "Mechanical and physical properties of cellular lightweight concrete block masonry." *Construction and Building Materials*, 248, 118621.

BS EN 1052-3 (2002). "Methods of test for masonry. Determination of initial shear strength." British Standards Institution, London.

Celarec, D., Ricci, P., and Dolsek, M. (2012). "The sensitivity of seismic response parameters to the uncertain modelling variables of masonry-infilled reinforced concrete frames." *Engineering Structures*, 35, 165-177.

Celik, O. C., and Ellingwood, B. R. (2010). "Seismic fragilities for non-ductile reinforced concrete frames–Role of aleatoric and epistemic uncertainties." *Structural Safety*, 32(1), 1-12.

Chandrappa, A. K., and Biligiri, K. P. (2017). "Flexural-fatigue characteristics of pervious concrete: Statistical distributions and model development." *Construction and Building Materials*, 153, 1–15.

Chen, X., Wu, S., and Zhou, J. (2014). "Variability of compressive strength of concrete cores." *Journal of Performance of Constructed Facilities*, 28(4), 06014001.

Cornell, C. A., Jalayer, F., Hamburger, R. O., and Foutch, D. A. (2002). "Probabilistic basis for 2000 SAC federal emergency management agencysteel moment frame guidelines." *Journal of Structural Engineering,* 128 (4), 526–533.

Crisafulli F. J. (1997). "Seismic behaviour of reinforced concrete structures with masonry infills." *Ph.D. Thesis*, University of Canterbury, New Zealand.

Dhir, P. K., Zade, N. P., Basu, A., Davis, R., and Sarkar, P. (2020). "Implications of importance factor on seismic design from 2000 SAC-FEMA perspective." *ASCE-ASME Journal of Risk and Uncertainty in Engineering Systems, Part A: Civil Engineering*, 6(2), 04020016.

EasyFit version 5.6 (Computer software), MathWave technologies, dnepropetrovsk, Ukraine. Mathwave, Available at: http://www.mathwave.com/.

Ellingwood, B., and Tallin, A. (1985). "Limit states criteria for masonry construction." *Journal of Structural Engineering*, 111(1), 108-122.

Fardis, M. N. (1996). "Experimental and numerical investigations on the seismic response of RC infilled frames and recommendations for code provisions." *Laboratorio Nacional de Engenharia Civil*, Lisbon, Portugal.

FEMA P-695 (2009). "Quantification of building seismic performance factors." Federal Emergency Management Agency, Washington, D.C.

FEMA-356 (2000). "Prestandard and commentary for the seismic rehabilitation of buildings." Federal Emergency Management Agency, Washington, D.C.

Haran, P. D., Davis, R., and Sarkar, P. (2015). "Reliability evaluation of RC frame by two major fragility analysis methods." *Asian Journal of Civil Engineering*, 15(1), 47-66.

IS 1893 (2016). "Criteria for earthquake resistant design of structures. Part 1: General provisions and buildings." Bureau of Indian Standards, New Delhi, India.

IS 456 (2000). "Plain and reinforced concrete - code of practice." Bureau of Indian Standards, New Delhi, India.

IS 875 (1987). "Code of practice for design loads (other than earthquake) for buildings and structures. Part 1: Dead loads - unit weights of building materials and stored materials." Bureau of Indian Standards, New Delhi, India.

Jones, M. R., and McCarthy, A. (2005). "Preliminary views on the potential of foamed concrete as a structural material." *Magazine of Concrete Research*, 57(1), 21–31.

Jos R., and Llukito, M. (2011). "Influence of water absorption on properties of AAC and CLC lightweight concrete brick." *4th ASEAN Civil Engineering Conference*, Yogyakarta, Indonesia.

Kearsley, E.P., and Wainwright, P. J. (2002). "The effect of porosity on the strength of foamed concrete." *Cement and Concrete Research*, 32(2), 233–239.

Kilinc, K., Celik, A. O., Tuncan, M., Tuncan, A., Arslan, G., and Arioz, O. (2012). "Statistical distributions of in-situ micro core concrete strength." *Construction and Building Materials*, 26 (1), 393–403.

Lawrence, S. J. (1985). "Random variations in brickwork properties." *7th Int. Brick Masonry Conf.,* 537–547. University of Melbourne, Australia.

Mamun, A. A., and Saatcioglu, M. (2017). "Seismic fragility curves for reinforced concrete framebuildings in Canada designed after 1985." *Canadian Journal of Civil Engineering*, 44, 558–568.

McKenna, F. (2016). OpenSees [Computer software], Pacific Earthquake Engineering Center a framework for earthquake engineering simulation. *Univ. of California, Berkeley, CA.< http://opensees. berkeley. edu/>(Dec. 16, 2018)*.

Mistri, A., Sarkar, P., and Davis, R. (2019). "Column–beam moment capacity ratio and seismic risk of reinforced concrete frame building." *Proceedings of the Institution of Civil Engineers – Structures and Buildings*, 172(3), 189–196.

Montazerolghaem, M. (2015). "Analysis of unreinforced masonry structures with uncertain data." *Ph.D. Thesis*, Dept. of Civil and Architecture, Technische Universität Berlin, Germany.

Nath, S. K., and Thingbaijam, K. K. S. (2012). "Probabilistic seismic hazard assessment of India." *Seismological Research Letters*, 83(1), 135-149.

Rasheed, M. A. (2018). "Mechanical characterisation of fiber reinforced cellular lightweight concrete for structural application of masonry." *Ph.D. Thesis*, Dept. of Civil Engineering, Indian Institute of Technology Hyderabad, India.

RILEM (1993). "Autoclaved aerated concrete - Properties, testing and design", *Taylor and Francis*, London, UK.

Sahoo, K., Dhir, P. K., Teja, P. R. R., Sarkar, P., and Davis, R. (2020). "Variability of silica fume concrete and its effect on seismic safety of reinforced concrete buildings." *Journal of Materials in Civil Engineering*, 32(4), 04020024.

Sahu, S., Sarkar, P., and Davis, R. (2019). "Quantification of uncertainty in compressive strength of fly ash brick masonry." *Journal of Building Engineering*, 26, 100843.

Sahu, S., Sarkar, P., and Davis, R. (2020). "Uncertainty in bond strength of unreinforced fly-ash brick masonry." *Journal of Materials in Civil Engineering*, 32(3), 06020003.

Schueremans, L. (2001). "Probabilistic evaluation of structural unreinforced masonry." *Ph.D. thesis*, Dept. of Civil Engineering, Catholic Univ. of Leuven, Belgium.

Singhal, V., and Rai, D. C. (2014). "Suitability of half-scale burnt clay bricks for shake table tests on masonry walls." *Journal of Materials in Civil Engineering*, 26(4), 644-657.

Sorrentino, L., Infantino P., and Liberatore D. (2016). "Statistical tests for the goodness of fit of mortar compressive strength distributions." *16th Int. Brick and Block Masonry Conf.* (IBMAC), 1921–1928. Taylor & Francis Group, Rome.

Stephens, M. A. (1974). "EDF statistics for goodness of fit and some comparisons." *Journal of the American Statistical Association*, 69(347), 730-737.

Stewart, M. G., and Lawrence S. J. (2007). Model error, structural reliability and partial safety factors for structural masonry in compression. *Masonry international*, 20 (3), 107–116.

Vamvatsikos, D. (2013). "Derivation of new SAC/FEMA performance evaluation solutions with second-order hazard approximation." *Earthquake Engineering & Structural Dynamics*, 42(8), 1171-1188.

Vamvatsikos, D., and Cornell, C. A. (2002). "Incremental dynamic analysis." *Earthquake Engineering & Structural Dynamics*, 31(3), 491-514.

Wijaya, H., Rajeev, P., Gad, E., and Amirsardari, A. (2020). "Effect of Infill-Wall Material Types and Modeling Techniques on the Seismic Response of Reinforced Concrete Buildings." *Natural Hazards Review*, 21(3), 04020031.

Yue, L., and Bing, C. (2014). "New type of super-lightweight magnesium phosphate cement foamed concrete." *Journal of Materials in Civil Engineering*, 27(1), 04014112.

All Tables

Table 1: Statistics and percentile values of compressive and shear-bond strength data (in MPa)

Statistics	f_m	τ_{cr}	Percentile	f_m	τ_{cr}
Sample Size	20	20	Min	1.315	0.150
Range	2.247	0.3	5%	1.344	0.151
Mean	2.4265	0.23625	10%	1.916	0.163
Variance	0.26215	0.0048	25% (Q1)	2.038	0.191
Std. Deviation	0.512	0.069	50% (Median)	2.434	0.218
Coef. of Variation	0.211	0.293	75% (Q3)	2.794	0.250
Std. Error	0.114	0.015	90%	3.163	0.335
Skewness	0.150	1.699	95%	3.543	0.444
Excess Kurtosis	0.521	3.841	Max	3.562	0.450

Table 2: Parameters for selected probability distribution functions

Masonry	Property	Distribution	Parameters
CLC	Compressive strength	Normal	μ =2.426, σ =0.512
		Lognormal	μ =0.864, σ =0.215
		Gamma	α =0.108, β =22.459
		Weibull	α =2.570, β =5.1409
		Gumbel max	μ =2.196, σ =0.399
		Gumbel min	μ =2.657, σ =0.340
	Shear-bond strength	Normal	μ =0.236, σ =0.069
		Lognormal	μ =-1.477, σ =0.254
		Gamma	α =11.626, β =0.020
		Weibull	α =4.942, β =0.245
		Gumbel max	μ =0.205, σ =0.054
		Gumbel min	μ =0.267, σ =0.054

Note: μ= continuous location parameters, α= continuous shape parameters, and β, σ = continuous scale parameters

Table 3: GOF test result for compressive strength of CLC block masonry

Distribution	KS		AD		CS		Total statistics
	Statistic	Rank	Statistic	Rank	Statistic	Rank	
Normal	0.107	2	0.261	1	0.453	5	0.534
Lognormal	0.108	3	0.320	3	0.140	2	0.365
Gamma	**0.105**	**1**	**0.277**	**2**	**0.182**	**3**	**0.348**
Weibull	0.146	5	0.376	4	0.357	4	0.539
Gumbel max	0.123	4	0.508	5	0.131	1	0.540
Gumbel min	0.152	6	0.760	6	1.780	6	1.941

Table 4: GOF test result for shear-bond strength of CLC block masonry

Distribution	KS		AD		CS		Total statistics
	Statistic	Rank	Statistic	Rank	Statistic	Rank	
Normal	0.221	5	0.911	4	2.020	5	2.226
Lognormal	0.160	3	0.385	2	0.579	2	0.713
Gamma	0.185	4	0.582	3	0.645	4	0.889
Weibull	0.129	1	1.514	5	0.603	3	1.634
Gumbel max	**0.153**	**2**	**0.359**	**1**	**0.362**	**1**	**0.532**
Gumbel min	0.284	6	2.766	6	7.582	6	8.076

Table 5: Design details of selected RC building frame

Member	Storey number	Width × Depth (mm)	Longitudinal reinforcement	Transverse reinforcement
Column	1	450×450	16-28 φ (UD)	10 φ @ 200 mm c/c
	2-3	450×450	16-25 φ (UD)	10 φ @ 200 mm c/c
	4-8	450×450	8-25 φ (UD)	10 φ @ 200 mm c/c
Beam	1-6	300×400	5- 25 φ (T) +3-25 φ (B)	10 φ @ 175 mm c/c
	7	300×400	4- 25 φ (T) +3-25 φ (B)	10 φ @ 175 mm c/c
	8	300×400	3- 25 φ (T) +2-25 φ (B)	10 φ @ 175 mm c/c

Note: UD= uniformly distributed, T= top rebar, B= bottom rebar

Table 6. Probability distribution of selected infill masonry

Masonry	Parameters	Shape Parameter	Scale Parameter	Distribution	Reference
CLC	Compressive strength, f_m	0.865	22.45	Gamma	Present study
		2.426	0.512	Normal	Assumed
	Shear-bond strength, τ_{cr}	0.205	0.054	Gumbel max	Present study
		0.236	0.069	Normal	Assumed
Clay	Compressive strength, f_m	5.320	0.800	Normal	Singhal and Rai, 2014
	Shear-bond strength, τ_{cr}	0.430	0.100	Normal	
Fly-ash	Compressive strength, f_m	3.900	0.580	Normal	Basha and Kaushik, 2015
	Shear-bond Strength, τ_{cr}	0.460	0.092	Normal	

Table 7: Other physical and mechanical properties of selected infill masonry

Materials	Parameters	Mean	Reference
CLC Block Masonry	Density (kg/m^3)	602.75	Bhosale *et al.,* 2020
	Modulus of elasticity (MPa)	990 f_m	Bhosale *et al.,* 2020
Clay Brick Masonry	Density (kg/m^3)	1773.50	Singhal and Rai, 2014
	Modulus of elasticity (MPa)	620 f_m	Ellingwood, 1985
Fly-ash Brick Masonry	Density (kg/m^3)	1660.00	Basha and Kaushik, 2016
	Modulus of elasticity (MPa)	600 f_m	Basha and Kaushik, 2015
Reinforced Concrete	Density (kg/m^3)	2500.00	IS 875 (Part-1): 1987
	Modulus of elasticity (MPa)	$5000\sqrt{f_{ck}}$	IS 456: 2000

Table 8: Calculation of design base shear of selected RC frame with different infill

Infilled frames	Seismic weight W (kN)	$T_1(s)$	Design base shear V_b (kN)
CLC	7698	0.67	709
Clay	10151	0.61	1016
Fly-ash	9865	0.59	1010

Table 9: PSDMs of the selected infilled frames

Frame with masonry type	ISD (%)	$\beta_{D\|IM}$	R^2
CLC_BF	1.128 $(S_{a,T1})^{1.043}$	0.358	0.785
CLC_ND	1.190 $(S_{a,T1})^{1.075}$	0.323	0.814
Clay	0.945 $(S_{a,T1})^{1.09}$	0.301	0.843
Fly-ash	0.951 $(S_{a,T1})^{1.121}$	0.275	0.875

Note: $S_{a,T1}$ is in terms of the gravitational acceleration (g)

Table 10: Fragility percentiles for RC frame infilled with different masonry

Infill type	Performance level	Fragility percentiles in terms of $S_{a,T1}$ (g)		
		25th	50th	75th
CLC_ND	IO	0.612	0.850	1.200
	LS	1.150	1.625	2.275
	CP	2.200	3.100	4.350
CLC_BF	IO	0.625	0.900	1.275
	LS	1.200	1.725	2.475
	CP	2.350	3.375	4.825
Clay	IO	0.775	1.075	1.475
	LS	1.437	2.000	2.750
	CP	2.700	3.750	5.200
Fly-ash	IO	0.775	1.050	1.425
	LS	1.425	1.950	2.650
	CP	2.650	3.600	4.925

Table 11: Probability of collapse P_{PL} ($\times 10^{-3}$) of selected RC frame infilled with different masonry

Masonry type	Limit state capacities		
	IO	LS	CP
CLC_BF	5.528 (1.00)	1.550 (1.00)	0.354 (1.00)
CLC_ND	5.835 (1.06)	1.684 (1.08)	0.380 (1.09)
Clay	4.522 (0.81)	1.305 (0.84)	0.315 (0.89)
Fly-ash	4.683 (0.84)	1.361 (0.87)	0.333 (0.94)

Figure 1

Click here to access/download;Figure;Fig. 1.tif

Variability of mechanical properties of cellular lightweight concrete infill and its effect on seismic safety

Figure 2

Click here to access/download;Figure;Fig. 2.tif

Variability of mechanical properties of cellular lightweight concrete infill and its effect on seismic safety

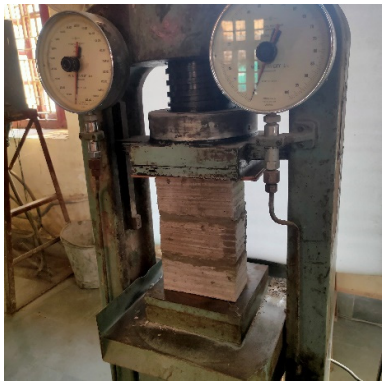

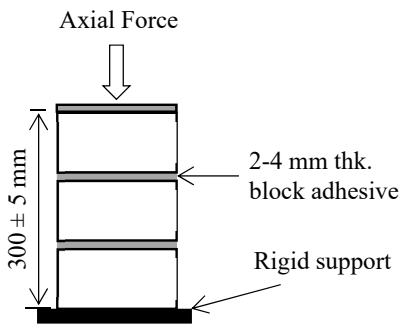

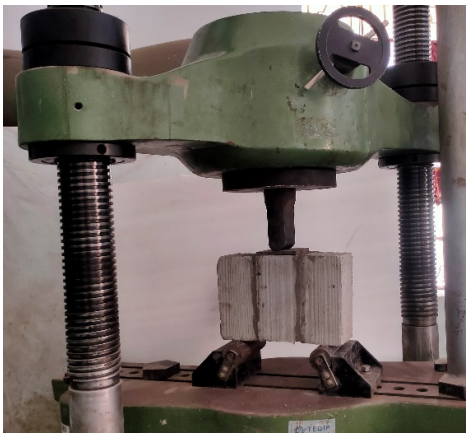

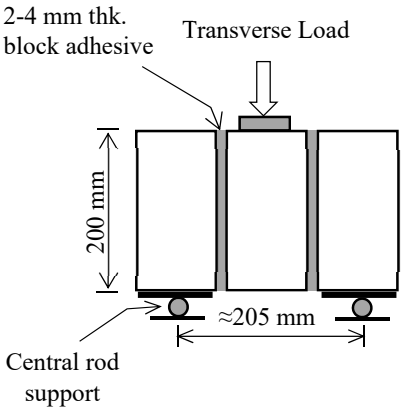

Variability of mechanical properties of cellular lightweight concrete infill and its effect on seismic safety

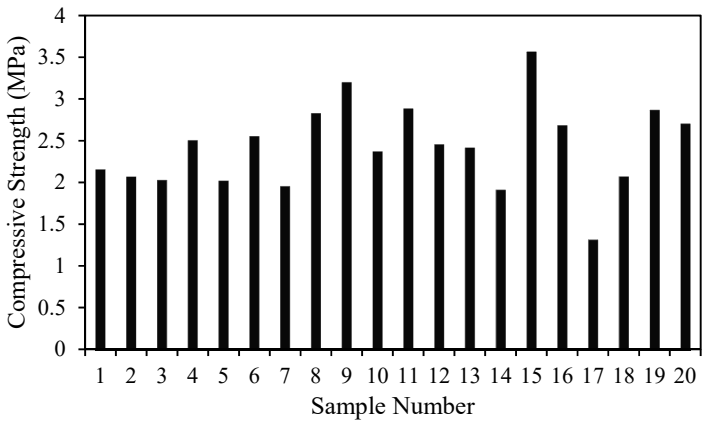

Variability of mechanical properties of cellular lightweight concrete infill and its effect on seismic safety

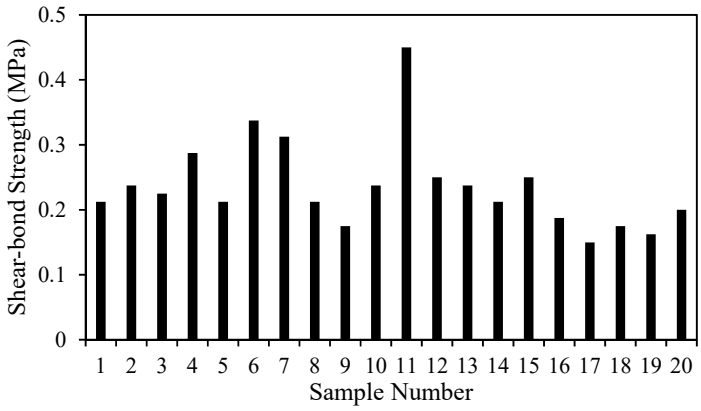

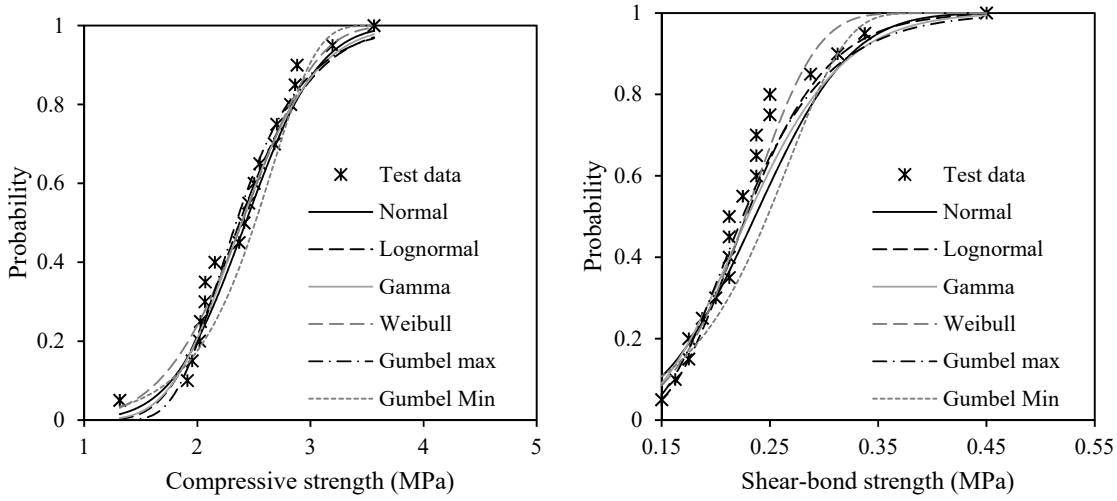

(a) (b)

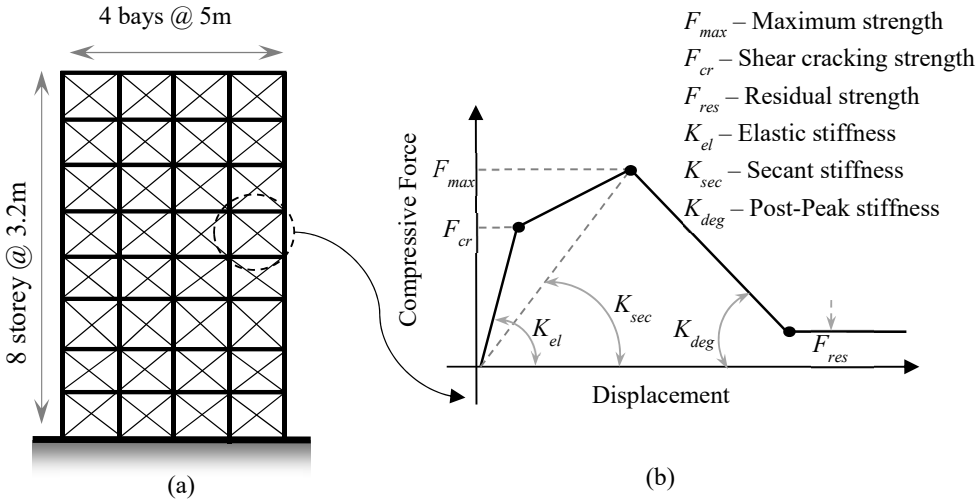

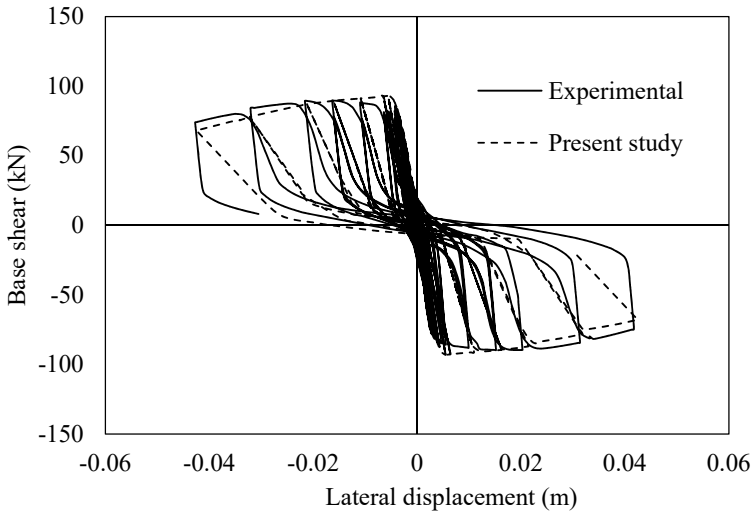

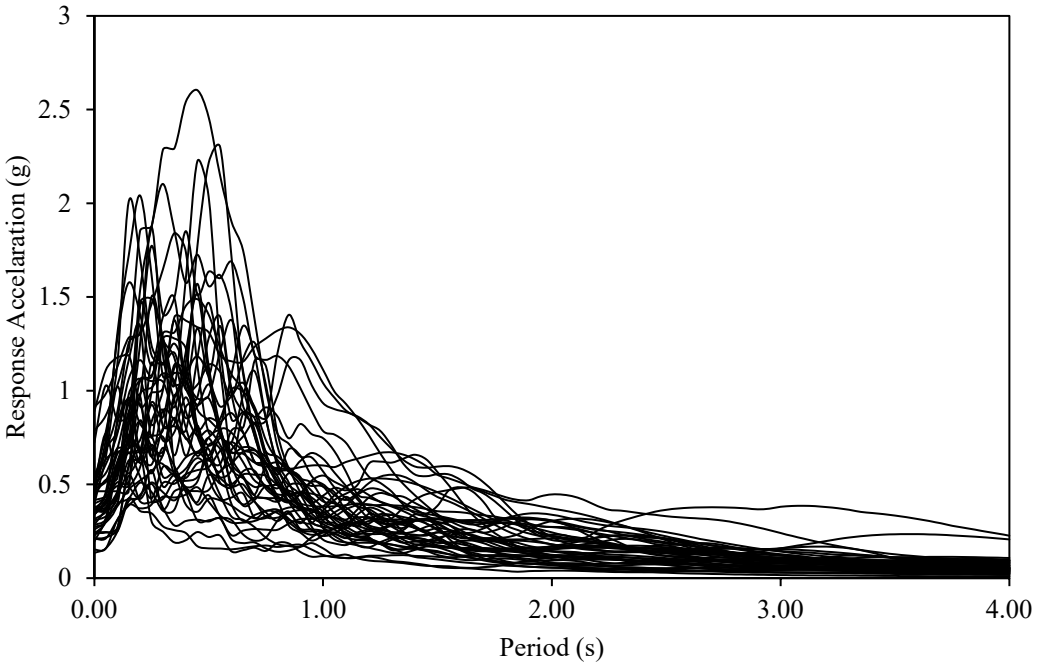

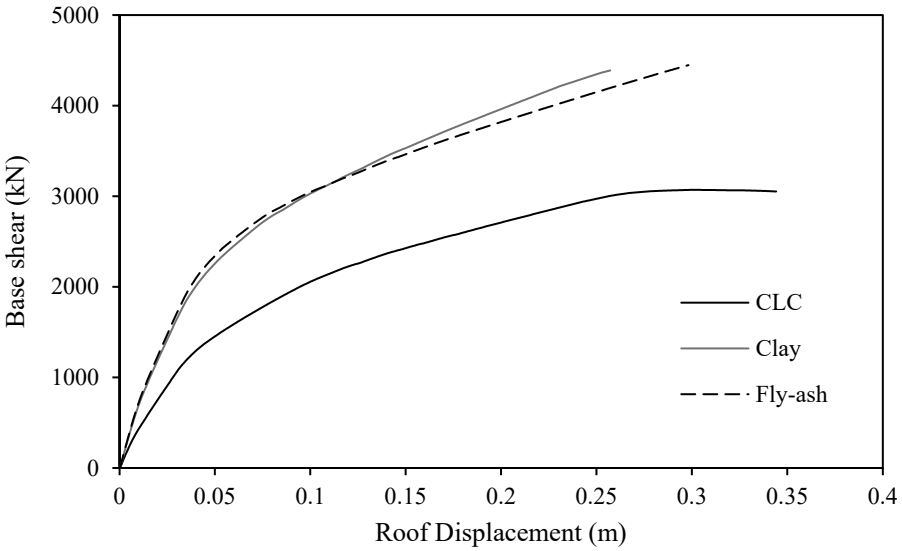
5000
4000
3000
2000
1000
0
Base shear (kN)
0
0.05
0.1
0.15
0.2
0.25
0.3
0.35
0.4
Roof Displacement (m)
CLC
Clay
Fly-ash

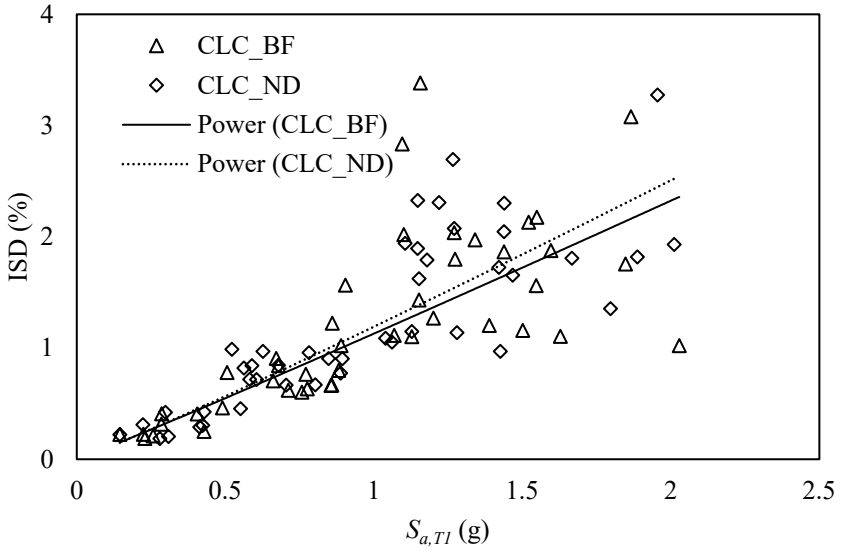
CLC_BF
CLC_ND
Power (CLC_BF)
Power (CLC_ND)
ISD (%)
0
1
2
3
4
0
0.5
1
1.5
2
2.5
$S_{a,T1}$ (g)

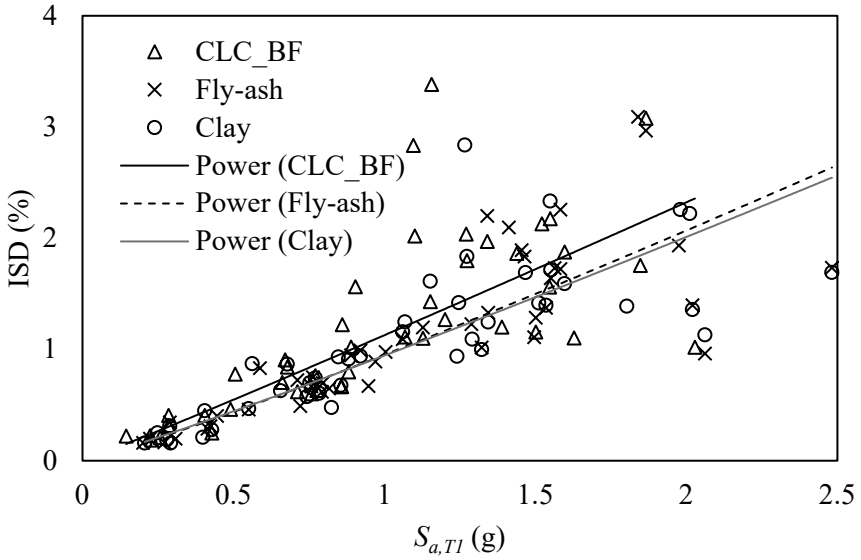
CLC_BF
Fly-ash
Clay
Power (CLC_BF)
Power (Fly-ash)
Power (Clay)
ISD (%)
$S_{a,T1}$ (g)
0
1
2
3
4
0
0.5
1
1.5
2
2.5

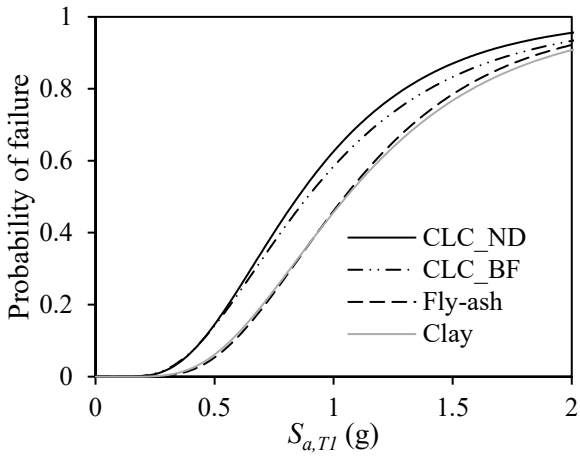
Probability of failure
1
0.8
0.6
0.4
0.2
0
0
0.5
1
1.5
2
$S_{a,T1}$ (g)
CLC_ND
CLC_BF
Fly-ash
Clay

(a) IO

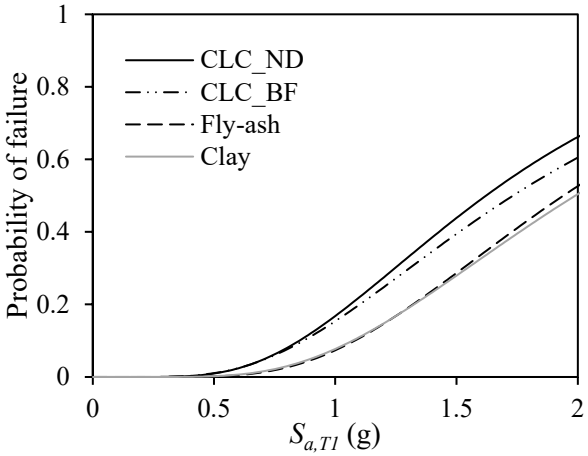
Probability of failure
1
0.8
0.6
0.4
0.2
0
0
0.5
1
1.5
2
$S_{a,T1}$ (g)
CLC_ND
CLC_BF
Fly-ash
Clay

(b) LS

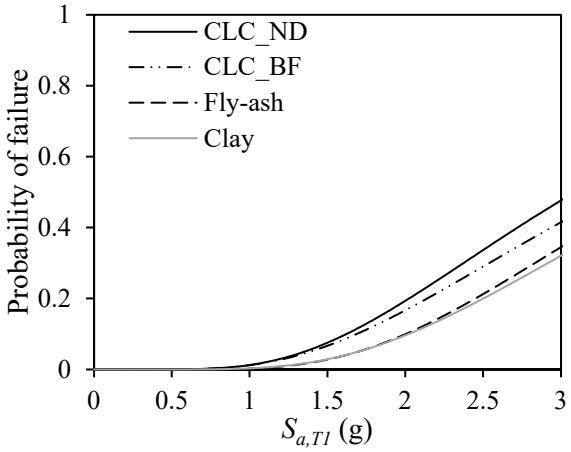
Probability of failure
1
0.8
0.6
0.4
0.2
0
0
0.5
1
1.5
2
2.5
3
$S_{a,T1}$ (g)
CLC_ND
CLC_BF
Fly-ash
Clay

(c) CP

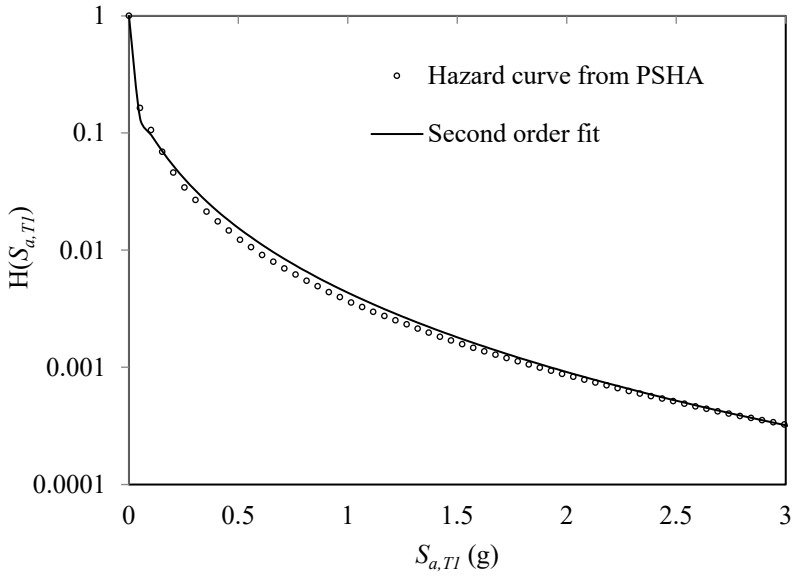
1
0.1
0.01
0.001
0.0001
H($S_{a,T1}$)
0
0.5
1
1.5
2
2.5
3
$S_{a,T1}$ (g)
Hazard curve from PSHA
Second order fit

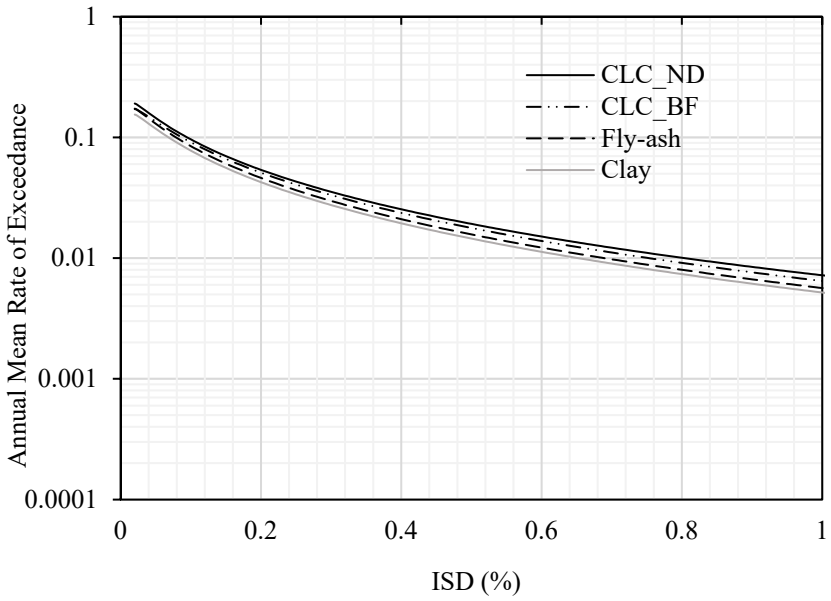

List of Figures:

Fig. 1: Procured CLC blocks

Fig. 2: Prepared CLC block masonry triplet specimens

Fig. 3: Test setup for compressive and shear-bond strength (a) Compressive strength test

(b) Shear-bond strength test

Fig. 4: Compressive strength values of all tested masonry specimens

Fig. 5: Shear-bond strength values of all tested masonry specimens

Fig. 6: Cumulative probability distributions for CLC block masonry triplets (a) Compressive strength and (b) Shear-bond strength

Fig. 7: (a) Geometry of selected building frame and (b) Backbone curve for the infill strut element

Fig. 8: Comparative plot of the building response obtained from the experiment and analysis

Fig. 9: Response spectra of selected ground motion records

Fig. 10: Pushover curves of selected RC frame infilled with different masonry materials

Fig. 11: PSDMs of CLC infilled frame with different distribution

Fig. 12: PSDMs of RC frame infilled with different masonry materials

Fig. 13: Fragility curves of RC frame infilled with different masonry at selected limit states

Fig. 14: Typical $S_{a,T1}$ hazard curve for $T_1 = 0.67$ s at Guwahati, India and its second-order fit via Eq. (3)

Fig. 15. Drift hazard curves of RC frame infilled with different masonry materials